Sliding Window along with EEGNet based Prediction of EEG Motor Imagery

Pabba Saideepthi, Anirban Chowdhury, *Member, IEEE*, Pramod Gaur, *Member, IEEE*, Ram Bilas Pachori, *Senior Member, IEEE*

***Abstract*—The need for repeated calibration and accounting for inter-subject variability is a major challenge for the practical applications of a brain-computer interface. The problem becomes more challenging while decoding the brain signals of stroke patients due to altered neurodynamics caused by lesions. Recently, several deep learning architectures came into the picture although they often failed to produce superior accuracy as compared to the traditional approaches and mostly do not follow an end-to-end architecture as they depend on custom features. However, a few of them have the promising ability to create more generalizable features in an end-to-end fashion such as the popular EEGNet architecture. Although EEGNet was applied for decoding stroke patients' motor imagery (MI) data its performance was as good as the traditional methods. [1] In this study, we have augmented the EEGNet-based decoding by introducing a post-processing step called the longest consecutive repetition (LCR) in a sliding window-based approach and named it EEGNet+LCR. The proposed approach was tested on a dataset of 10 hemiparetic stroke patients' MI data set yielding superior performance against the only EEGNet and a more traditional approach such as common spatial pattern (CSP)+support vector machine (SVM) for both within- and cross-subject decoding of MI signals. We also observed comparable and satisfactory performance of the EEGNet+LCR in both the within- and cross-subject categories which are rarely found in literature making it a promising candidate to realize practically feasible BCI for stroke rehabilitation.**

***Index Terms*—Brain-computer interface, EEG, motor-imagery, EEGNet, Deep learning, CNN, neurorehabilitation.**

I. Introduction

One of the first attempts to use deep convolutional neural network (CNN) for motor imagery (MI) classification was made by Sakhavi et al. [2] where they used parallel linear convolution with dynamic energy features to classify Brain-computer interface competition (BCIC) IV-2a dataset. This approach achieved a significantly better average accuracy of 70.6% over support vector machine (SVM) with static energy features although a comparison with the state-of-the-art filter bank common spatial pattern (FBCSP) [3] was not given. L Zheng et al. [4] proposed the PSPD method to improve the classification performance of MI which achieves an average classification accuracy of 84.51%, 84.10%, and 73.21% in BCI Competition IV Dataset IIa, Dataset IIb and OpenBMI dataset, respectively. Another study, done by Lu et al. [5] used restricted Boltzmann machine (RBM) on frequency domain features of EEG to classify MI dataset of BCI Competition IV-2b which showed significant improvement over FBCSP with an average classification accuracy of 84% although the kappa values were not reported as in [3]. Qun He et al. [6] proposed M2NN and MTL model to improve the recognition rate and generalization ability of MI with the fusion of EEG. This approach achieved an average accuracy of 82.11% across 29 subjects. Tang and Sun [7] used an in-house MI EEG dataset of only two subjects to evaluate their deep CNN architecture and hence comparison with the existing state-of-the-art was not possible. At the same time, another work was done by Taber and Halici [8] where they used CNN with stacked autoencoders (CNN-SAE) on the BCI Competition IV-2b dataset to produce the results. The average kappa value reported for 10-fold cross-validation on all sessions was 0.547 which was slightly higher than the state-of-the-art FBCSP algorithm [3] with an average kappa value 0.502. However, the session-to-session accuracy in the case of FBCSP increased to 0.6 (winner of the competition) while in the case of CNN-SAE the performance was reported to be decreased from the average accuracy of 77.6% in 10-fold cross-validation on all sessions to 75.1% in session-to-session transfer. This makes the superiority of CNN-SAE inconclusive over FBCSP. Unlike these two works ([7], [8]) where the spatiotemporal features were used as inputs, Schirrmeister et al. [9] used deep (dCNN) and shallow CNN (sCNN) architectures to learn the features which led to some improvement over the existing results on BCIC IV-2a and 2b datasets. Interestingly, the shallow CNN performed better than deep CNN and FBCSP, achieving average decoding accuracy of 73.7% (+5.7% than FBCSP; P-value$<$0.05) in BCIC IV-2a dataset and average kappa of 0.629 (+0.03 than FBCSP) in BCIC IV-2b while deep CNN could only match the results of FBCSP. Overall, this work at least established CNNs as a promising choice for end-to-end MI decoding without depending on hand-crafted features such as spatio temporal images. Another work was done by T Shi et al. [10] for EEG feature extraction algorithm based on common spatial pattern (CSP) and adaptive auto-regressive (AAR) used for motor imagery classification, the simulation results show that when a certain kind of motor imagery is performed, the probability of the corresponding characteristic signal value is the smallest. The robustness of BCI decoding has also been improved by the application of novel time

Manuscript received XXXX XX, 2021; revised XXXX XX, 2021.

(Corresponding author: Pramod Gaur.)

P.Saideepthi is with the Department of Computer Science, BITS Pilani Dubai Campus, UAE (e-mail: p20200901@dubai.bits-pilani.ac.in), P. Gaur is with the Department of Computer Science, BITS Pilani Dubai campus, UAE (e-mail: pgaur@dubai.bits-pilani.ac.in). A. Chowdhury is with School of Computer Science and Electronic Engineering, University of Essex, Colchester, CO4 3SQ, UK (e-mail: a.chowdhury@essex.ac.uk). R. B. Pachori is with the Department of Electrical Engineering, IIT Indore, Indore, India (pachori@iiti.ac.in).

filters applied for SSVEP classification [11]. Feature selection methods are also proposed to handle the non-stationarity in EEG signals [12]. Some researchers took the approach of combining different modalities such as P300 and SSVEP in a hybrid-BCI fashion to enhance performance [13]. In another study, done by Q Yao, H Gu et al. [14] to process the 3-D features for EEG emotion recognition, participant-dependent and Participant-independent protocols are conducted to evaluate the performance which yielded accuracies of 89.67% and 79.45%. The next important development in deep learning-based BCI was the creation of EEGNet architecture by Lawhern et al. [15] which explored the possibility of a generalized compact CNN architecture across different BCI paradigms including MI on BCIC-2a dataset. For within-subject classification, the proposed EEGNet-8,2 architecture performed equally well as FBCSP although the accuracies were reported on a 4-fold cross-validation and not session-to-session transfer. The study also found similar observation as in [9] where a shallow CNN performed better than deep CNN in within-subject case. However, in the cross-subject case, all the CNN architectures (DeepCNN, ShallowCNN, and EEGNet-8,2) gave a comparable performance while only a marginal (not significant) improvement over FBCSP was observed. Moreover, as the session-to-session performance was not reported in this study, a direct comparison with the previous results on BCIC-2a dataset is not possible. Sakhavi et al. [16] futher developed their CNN model to propose channel-wise convolution with channel mixing (C2CM) which led to significant improvement of around 7% over FBCSP on BCIC IV-2a dataset with average decoding accuracy of 74.46% (kappa = 0.659). This was one of the first evidence where a CNN-based approach comprehensively outperformed the state-of-the-art. However, the effectiveness of a deep learning-based approach for cross-subject or inter-subject decoding of MI signals was still unknown as EEGNet-8,2 [15], the only method that dealt with the problem till then, achieved limited success. Cross-subject decoding is important to explore as it is one of the potential options to realize calibration-free BCI as existing BCI designs are heavy in recalibration needs which ultimately hinders their way for practical uses. [17] presents a novel technique for the classification of motor imagery (MI) electroencephalogram (EEG) signals employing a multiplex weighted visibility graph (MWVG) algorithm with an average classification accuracy of 99.92% and 99.96% is obtained using the Random Forest classifier. Dagois et al. [18] introduced a multimodal hybrid BCI based on electroencephalography (EEG) and functional transcranial Doppler ultrasound (fTCD) and present a TL approach to reduce the calibration requirements. The first successful application of a deep learning-based approach for cross-subject decoding was done by Kwon et al. [19] who used a large MI dataset of 54 subjects to show that their proposed CNN framework with spectral-spatial input outperformed several existing cross-subject decoding approaches including FBCSP. Motor Imagery (MI) classification is one of the major contributions in BCI which works on a segment of EEG signal within a particular frequency band, S Mohidwale [20] introduced the Harmony search algorithm of feature selection to obtain the optimal feature set for the classification of MI with an average accuracy of 92.49%. Despite the success on cross-subject decoding the method only gave a comparable performance for within-subject decoding. Moreover, the results were only compared with the traditional methods and not with the pre-existing deep learning approaches such as EEGNet [15]. Continuous wavelet transform (CWT) was also used to generate time-frequency images as input to a simplified CNN (CWT-CNN) [21] which is claimed to have achieved the highest average kappa value of 0.651 so far on BCIC IV-2b dataset although the average accuracy (83.2%) was slightly lower than RBM [5] (84%). The reported kappa value was also higher than the CNN approach proposed in [9] (0.629). However, it is unclear whether they reported the session-to-session performance as only the cross-validation performances of other methods were considered for comparison in the paper. Olivas-Padilla and Chacon-Murguia [22] also claimed a very high average decoding accuracy (80.03%, kappa = 0.61) for BCIC IV-2a dataset by combining four expert CNNs into a modular network which was even higher than Sakhavi et al. [16] in terms of accuracy (74.46%) although the average kappa value was lower by 0.05. Dai et al. [23] argued about the dynamic change in the convolution scale which is often ignored in CNN-based MI classification and proposed hybrid-scale CNN (HS-CNN) to deal with this problem. This method argued about outperforming all the other state-of-the-art techniques (irrespective of traditional or deep learning-based methods) to classify both BCIC IV-2a and 2b datasets achieving average decoding accuracies of 91.57% and 87.6% respectively. However, it is worth noting that they reduced the problem in BCIC IV-2a to 2-class whereas originally it was a 4-class problem. So, the claim may not be verified at least for BCIC IV-2a dataset. An end-to-end framework for MI decoding was proposed by Li et al. [24] using channel project mixed-scale CNN (CP-MixedNet) which gave comparable average decoding accuracy (74.6%) to Sakhavi et al. [16] although the advantage is that CP-MixedNet uses raw EEG signals as input while in [16] an additional temporal feature extraction step is required using FBCSP. Similar performance (average kappa 0.64) on BCIC IV-2a was also achieved by Zhao et al. [25] by 3D representation of EEG signals in order to preserve the spatial and temporal features before feeding it to CNN. Tayeb et al. [26] proposed pragmatic CNN (pCNN) to classify the BCIC IV-2b dataset and compared it with dCNN and sCNN architectures given in [9]. Their study contradicted the outcome of [9] as dCNN was shown to have achieved the highest accuracy of 95.72% while sCNN (accuracy=78.22%) was not even close to that. Notably, the proposed pCNN achieved an accuracy of 91.63%. One of the few CNN models, employed for subject independent classification of MI signals, is a hybrid deep network combining CNN and long-term short-term memory (LSTM) network which uses FBCSP for feature extraction [27]. It achieved the highest performance so far in BCIC IV-2a dataset in the cross-subject category with average accuracy of 83% (kappa=0.80). In another approach involving deep recurrent neural networks with gated recurrent units (GRU-RNN) using the same FBCSP features Luo et al. [28] achieved an accuracy of 82.75% and 73.56% for BCIC IV-2a

and 2b datasets, respectively. Technical challenges, including signal pre-processing, spectrum analysis, signal decomposition, spatial filtering in particular canonical correlation analysis and its variations,and classification techniques for steady-state visual evoked potential (SSVEP)-based BCI system which uses multiple visual stimuli flickering at different frequencies [29]. The authors [30] P Autthasan et al. developed an integrated approach to simultaneously estimate the frequency and contrast-related amplitude modulations of the SSVEP signal. LASSO(least absolute shrinkage and selection operator) has achieved the highest average classification accuracy of 84.96% [31] a new EEG classification model implemented by S Zhang et al. used to model the group sparsity of EEG signals, the features of the same channel are assigned the same weights. Despite many notable works in the area of deep learning-based MI-BCI the application is mainly concentrated in the within-subject category while the cross-subject decoding is largely ignored in spite of being an important approach for realizing calibration-free BCI designs essential practical uses. Moreover, very few studies so far have addressed the problem of classifying stroke patients' MI data using deep learning which cannot be ignored as the major application area of MI-BCI is in rehabilitation. Therefore, in the current study, we tried to address these two problems together by testing the efficacy of deep learning in cross-subject decoding of MI signals on a stroke patient's dataset. We applied the EEGNet framework with a sliding window-based approach using the recently proposed longest consecutive repetition (SW-LCR) and mode (SW Mode) [32] based prediction named it (SW-EEGNet-LCR/Mode). The reason behind the choice of EEGNet architecture is that it is one of the most compact openly available CNN networks applied for MI decoding on healthy subjects, even for cross-subject category. Another important reason for choosing EEGNet is that it can learn the features directly from the raw data as we believe that one of the crucial advantages of using deep learning should be getting rid of the necessity of using hand-crafted features. The paper describes the performance of the proposed SW-EEGNet-LCR/Mode approach on an open-access stroke patient's dataset called 'Clinical BCI Challenge 2020 (CBCIC 2020)' [33] and on popular BCI Competition IV-2b dataset (for healthy subjects) to compares the results with the existing benchmarks and between the two subject categories.

II. Materials and Methods

A. Experimental design

The experiment follows a typical paradigm of a MI BCI based rehabilitation of stroke patients with two stages. The first stage is to acquire data without providing any feedback and was used to train a classifier with data obtained from this stage. In the second stage, online neurofeedback was provided based on the classifier's performance. The neurofeedback was concomitant and multimodal where both visual and proprioceptive feedback was provided. The visual feedback was a stop motion video on a computer screen showing a hand grasp action and concurrently the same motion was replicated on a hand-exoskeleton robot where the participant's impaired hand was attached. None of the stroke patients who participated in the experiment had prior experience using a BCI device. Data acquisition has two runs of 40 trials during the first stage i.e. the calibration stage while the online feedback consisted of one run of 40 trials. It takes about 7 minutes and 30 seconds to complete each run. The 40 trials within each run were equally divided between left and right-hand classes i.e. 20 right-hand class trials and 20 left-hand class trials. The gap between the calibration and online feedback stage was only 16 minutes, which was used to check the data and generate the classifier. This time gap is reasonable enough in a rehabilitation setting to assure that the patients do not lose focus during the experimentation. In the original experiment, the CSP features were used to train an SVM classifier for discriminating the two classes. The timing diagram of a particular trial in the online feedback stage can be found in Fig. 1 (a). The 40 trials in each run are equally divided between left and right-hand tasks to keep the chance level of prediction at 50%. The first 3 s after the start of the trial is the preparation phase where a 'Get Ready' cue is shown on the computer screen. Next, the cue for initiating the task appears on the screen which could be either left or right-hand imagery. This lasts for 5s till the end, if the trial during the training runs. The 'get ready' cue is provided as a text displayed on the computer screen for 3 s after a trial starts. The cues for the tasks are provided by showing pictures of a human hand with a curled-up posture to indicate that they need to make a grasp attempt. The task cues appeared either on the left or right of the screen depending on the left and right-hand classes. During the feedback stage, the task cue is replaced by the neurofeedback after 5s (from the start of the trial) to show a stop-motion video of a human hand, the aperture of which is controlled by the predicted labels issued every 0.5s until the end of the trial. The corresponding physical motion of the hand is provided with the exoskeleton. The time gap between the two consecutive trials can be between 2s to 3s. The EEG data was sampled at 512 Hz with a bandpass filter between 0.1-100 Hz cutoff frequencies while there was a notch filter to prevent the data affected by power supply noise of 50 Hz.

The exoskeleton used in this study is a lightweight, 3D printable, fully portable, and wearable exoskeleton with two degrees of freedom. The index and the middle fingers are driven in a coupled manner with a four-bar mechanism actuated by a servo motor. The thumb is driven separately by another four-bar mechanism with another servo motor. There are finger mounting caps at the end-effector of each of the arms of the exoskeleton to attach the fingertips. The forehand is supported by an armrest for gravity compensation and mounted on a tabletop during the experiment. The exoskeleton used in the experiment is shown in Fig. 2.

B. Dataset description

There are a total of 10 participants in the patient dataset (it is referred to as CBCIC2020 dataset in the rest of the paper). Each of them has a training file and a testing/evaluation file. These files contain information about the sampling rate (512 Hz), cue timing, the class labels corresponding to each

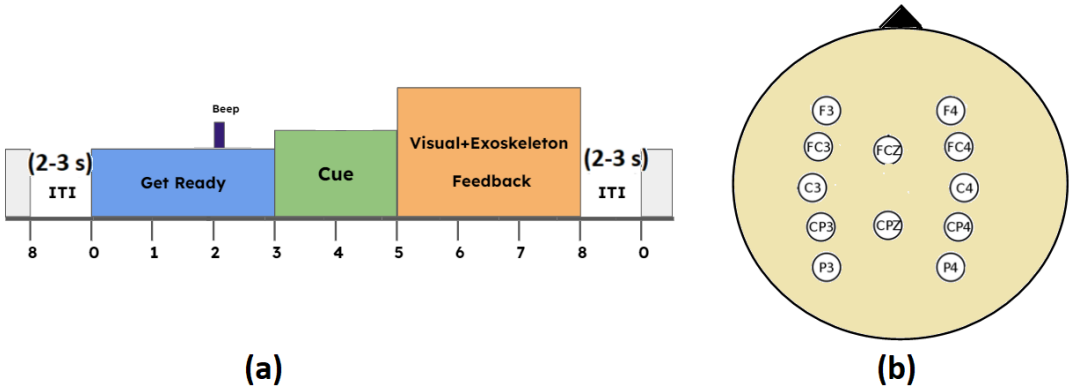

Fig. 1. (a) Timing diagram of the experimental paradigm involved in the dataset, (b) The EEG electrode placements. [34].

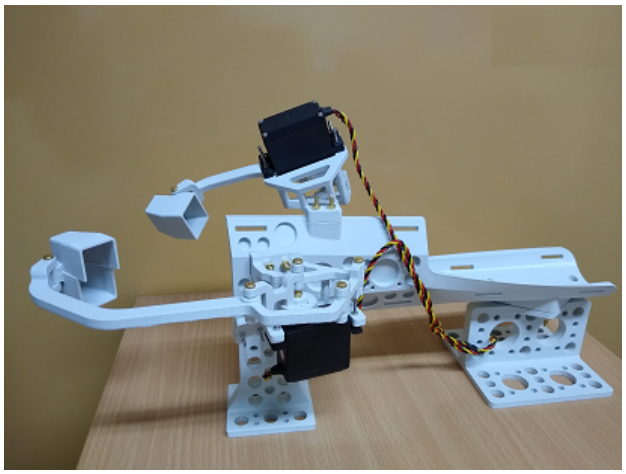

Fig. 2. Physical model of the two-degrees of freedom 3D printable exoskeleton used for the experiment.

trial, and the raw data across various trials and channels. For training, the raw data has 80 trials and for evaluation, it has 40 trials. There are altogether 12 EEG channels for both training and evaluation which are F3, FC3, C3, CP3, P3, FCz, CPz, F4, FC4, C4, CP4, and P4. Each trial contains 4096 samples (8s trial length $\times$ 512 Hz = 4096 samples).

We have also used a healthy subjects' dataset called BCI Competition IV-2b dataset[35] which is popular in the field of motor imagery BCI. This dataset is similar in configuration to the CBCIC2020 dataset as it also has two classes, left and right-hand imagery, and a trial length of 7.5 s. The sampling rate in this case is 250 Hz. There are 9 subjects in this dataset with several sessions of recording. We have used the first two sessions for training and the third session for testing just to keep parity with the CBCIC2020 dataset while comparing the results between the two.

C. EEGNet Architecture

EEGNet is one of the most popular deep learning architectures successfully used in BCI applications. EEGNet utilizes separable and depthwise convolutions for developing an EEG explicit model which confines well-known EEG feature extraction concepts for BCI. The number of trainable parameters are also very less in EEGNet for model prediction as compared to other commonly used deep learning architectures used in BCI classification. EEGNet is quite robust to learn a wide range of interpretable features over various tasks of BCI [15]. The data given was prone to overfitting therefore the EEGNet model has slightly been modified to suit the requirements of the dataset. For EEG trials, a 512 Hz sampling rate was used to collect the data over 12 channels. The description of the model can be defined in the following way [36]:

In the Block 1 there are two convolution steps starting with the input layer combining Conv2D and DepthwiseConv2D. In the first and second stages, each batch normalization is added after the 2D convolution and depthwise convolution accordingly. One of the advantages of using Depth wise convolution is that it can decrease the requirement of trainable parameters for fitting a deep predictive model. All the previous feature maps and depth-wise convolution are not fully connected. The spatial features can be learned from the combined Conv2D and depthwise Conv2D which directly corresponds to each temporal filter. This approach is influenced by the filter-bank standard spatial algorithm (FBCSP) technique while the number of spatial filters is regulated by the use of a depth parameter although, for each feature map, this parameter is to be learned.

Block 2 is related to separable convolution. In this block, a point-wise convolution is added after a depth-wise convolution to process the outputs from block-1. By using separable convolutions it is possible to further decrease the requirement of the parameters to fit the model. This method helps in summarizing the individual feature maps while point-wise convolution and depth-wise convolution helps in optimally combine the feature maps . This process also contributes to the representation of the feature maps according to the time scales.

In Block 3 a softmax function is used to process the features from the previous block to classify them into the left and right MI classes. Although EEGNet is capable of doing multiclass classification in the current scenario we have used it for binary classification only due to the nature of the dataset. This function is utilized here because EEGNet is a multi-class classification model.

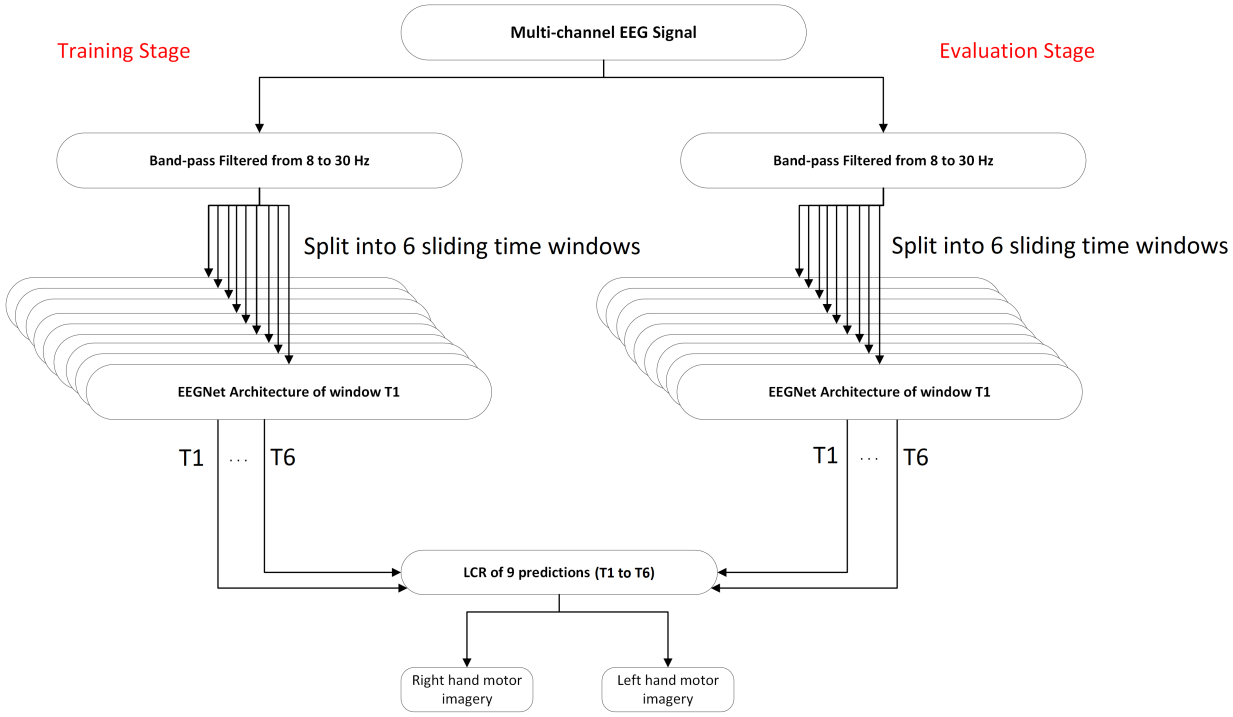

Fig. 3. Block diagram for the proposed method.

D. Sliding Window Process

As stated earlier in the experimental paradigm the trials are 8s long while the cue appeared 3s after the start of the trial, the time between 4s to 8s is considered for the windowing purpose. The timeline for the sliding windows started from 0.5 s after the cue (cue presented at 3s after the start of the trial). Each window is 2s and the shift between the two consecutive windows is 0.5s. Thus there are 6 windows in the timeline of the sliding windows which are as follows: 3.5s-5.5s, 4s-6s, 4.5s-6.5s, 5s-7s, 5.5s-7.5s, 6s-8s. The EEGNet was trained for each of these windows to generate 6 different models using the training dataset. While predicting the evaluation data with models corresponding to each of these windows are used to generate predicted labels. Then these predicted labels are passed into the longest consecutive repetition (LCR) function (described in section II.G) to decide the overall label of that particular trial; hence the single trial prediction is done. We also observed that the highest accuracy for the training data only was found at 4.5s-6.5s and 5s-7s. This information can be used to further reduce the computational complexity if someone wants to use only one EEGNet model to predict the labels of all the sliding windows in the evaluation data rather than using six different models for the corresponding windows. The number of time windows is chosen experimentally by keeping in mind its practical utility of it in case we need continuous feedback. In an earlier study, we issued continuous feedback with a shift of 0.5s between the two successive windows. Again, in order to extract meaningful features and bandpass filtering the window size should be long enough typically 1.5s to 2s long. Thus we fixed the shift as 0.5s and window size 2s. Then we started the windowing from 3.5s as the event-related desynchronization requires roughly 0.5s to hit the bottom (the cue was given at 3s; so, 3s+0.5s=3.5s). Hence, only 6 windows are possible with such constraints as the trial ends at 8s. It is to be noted that the validation set was 25% of the training data which means for each individual subject 20 out of 80 trials were used for validation (total trials in the training set was 80). The test data was a separate run of 40 trials; so it was unseen by the classifier.

E. Preprocessing

For passing the data into the EEGNet architecture the data is formatted into a 3D matrix format where (N, C, T) are three dimensions which are number of samples, number of channels, and number of trials accordingly. The lower and upper cutoff frequencies for the bandpass filtering was found by doing a grid search between 8 Hz-30 Hz and finally decided to be between 8 Hz and 24 Hz for optimal performance.

F. Model Parameters

A filter-size (kernel length) of 32 was used for the 2D convolution later in block 1 while the batch size was set to 16. The loss function was selected to be 'categorical cross-entropy' while the optimizer used in the process was 'adam'. For model building, the Keras and Tensorflow framework was used. We used Google colab with K80 Tesla GPU for generating the results.

G. SW-LCR

The sliding window-based longest consecutive repetition (SW-LCR) was used for post-processing the predictions from

EEGNet. The LCR is based on a sliding window-based approach where the EEG data from each window is classified by the classifier such as EEGNet and then we see the longest sequence of predicted labels in that series. For example, suppose there are 9 such EEG data windows within a trial and the EEGNet prediction for this sequence of windows is 122221122. Now out of these two predicted labels (right-hand class=1, left-hand class=2) the LCR is found for left-hand class=2 where 2 appeared consecutively 4 times. So, while classifying this particular trial into left or right-hand class, we will choose left-hand class=2. In case of a tie, i.e. both the classes has the same length of consecutive repetition, we choose the one which is observed first. For example, consider the prediction sequence 111122221. Here, both 1 and 2 have the same length of consecutive repetiton=4. Now, we can observe that the repetition of 1 occurred first and then 2. So, the predicted class for this trial would be right-hand class=1. The signal processing and machine learning pipeline along with the LCR-based post-processing of the single trial prediction is shown in Fig. 3. In this block diagram, we can see that both in the training and evaluation cases the EEG signal is band pass filtered between 8-30 Hz which signifies the sensory motor rhythm (SMR). This bandpass filtered signal is then used to train the EEGNet classifier in the training case which is then used in the evaluation case for predicting the sliding windows within the trial and then post-processing was done using the LCR technique for single trial prediction. There were altogether 9 successive data windows within the trial which started after 2s from the task initiation cue. This time gap is necessary for event-related desynchronization (ERD) to occur in the motor cortex which is the signature of the initiation of high-level motor command in the brain. Then these data windows run towards the end of the trial with a window length of 2s and overlap of 75%, i.e the shift between the two successive windows is 0.5s.

The SW-LCR operates as a post-processing step on the predictions by a classifier which makes it independent of the signal processing and machine learning pipeline before it. Because of this different feature extraction algorithms can be used in combination with SW-LCR. However, the advantage of using EEGNet+LCR is that it is an end-to-end process without the requirement of custom-made features. From the neurophysiological aspect the optimum time window within a trial varies significantly among the participants and also within a session. Therefore, many previous techniques of EEG decoding focused on finding the personalized time window of feature extraction. In contrast, LCR considers all the different time windows before making an overall judgment. This technique accounts for the variability within the session and across the participants in order to make a robust prediction. Moreover, when it comes to the question of stroke patients' EEG data the variability is much more due to altered neurodynamics caused by the lesion. Hence, EEGNet+LCR is especially relevant in this case as the EEGNet has the capacity to generate the features in a more personalized way as compared to hand-crafted features while the LCR manages the variability in the brain activation time window within a trial.

III. Results

The results from the CBCIC2020 dataset are obtained in two categories. The first one is the within-subject category where the EEGNet is trained using the same subject's training session and tested on the evaluation session of that subject only. The second one is the cross-subject category where a leave-one-out approach is adopted where the training sessions of all the other subjects are used to train EEGNet and then tested on the evaluation session of the left-out subject. It is worth mentioning that for single-trial-based prediction in the evaluation trials, LCR approach is used as mentioned in Section II-G. Additionally, we have provided the results on a popular healthy subjects' dataset called BCI Competition IV-2b for comparison purposes.

A. Within-subject decoding

The within-subject accuracies for individual subjects are reported in Table II. There are three different epochs for which the results are computed using different kernel lengths, while the bandpass frequency range ([8-24 Hz]) and dropout (0.25) are fixed. The kernel length for 100 epochs of training was 64 while it was 32 for both 300 epochs and 500 epochs of training. The highest average accuracy was observed for 500 epochs of training with 76.94% while the lowest average accuracy was in the case of 100 epochs of training with 69.26%. The standard deviation was also found to be the lowest at 13.5% in the case of 500 epochs. In the case of 300 epochs of training the performance was in the middle with an average accuracy of $72\pm14.47\%$. In 500 epochs case, 7 out of 10 subjects crossed the 70% accuracy mark which is often considered as a threshold for acceptable BCI performance while two of the subjects (S07 and S10) obtained more than 90% accuracy (92.5% and 94.5% respectively) and three more (S01, S02, and S08) achieved more than 80% accuracy (85%, 85%, and 82.5% respectively). It was also observed that for 500 epoch case, the accuracies of some of the low-performing subjects (S03 and S04) improved considerably.

The within-subject decoding performance for BCI Competition IV-2b dataset is presented in Fig. 5. The average accuracy for this dataset is found to be 77.71%. The highest accuracy was observed for subject B04 (98.75%), while 6 out of 9 of them achieved an accuracy of more than 75%.

B. Cross subject decoding

The cross-subject decoding was conducted following a leave-one-out methodology. This means we used the training data from all other subjects within the group leaving one of them from that group and then the trained classifier was used for testing the evaluation data from left out participant. For example, for calculating the cross-subject accuracy for participant S01, the training data from S02 to S10 was used for training the EEGNet and then it is used to decode the evaluation data for S01. The drop-out rate in this case is set to be 0.25. The average accuracies for different epoch sizes are shown in Table III. From the table, we can see that the average accuracy for 100 epochs is 67.5%, while for

300 and 500 epoch sizes they are 69.75% and 74.49%. The standard deviation of all these results varied between ±10.8% to ±14.33%.

A comparison between the classification accuracies of the proposed approach with the previous approaches on the same dataset is shown in Fig. 4 for both within- and cross-subject categories. This comparison has been discussed in detail in the discussion section.

We have also shown the variation in classification accuracy across all the subjects related to the choice of the number of windows for calculating the LCR in Table IV. As the number of windows is varied from 3 to 7 the accuracies are also varied for different subjects. For example, a significant improvement in accuracy is found for B09 when the number of windows is changed from 4 to 5 or more. A gradual improvement in accuracy is also found for B05 and B08 when the number of windows is incremented from 3 to 7. For B07 also the accuracy peaked when the number of windows is 5 or 6 although it dropped to 7. However, there is only moderate improvement in the accuracies when the number of windows is changed as seen by the mean and median scores at the bottom of Table IV.

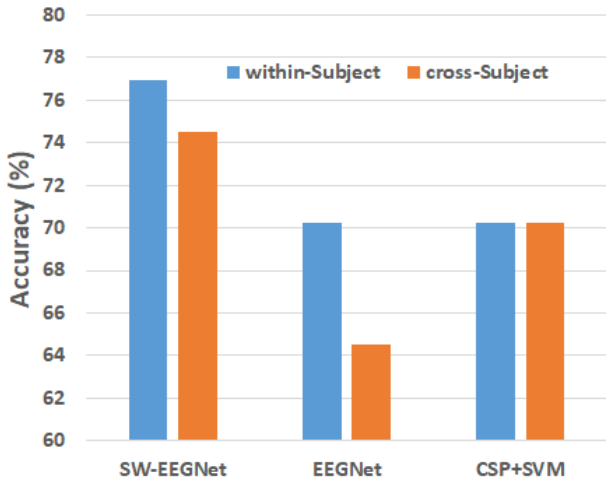

Fig. 4. Comparison of classification accuracies between different algorithms for the two categories: within-subject and cross-subject.

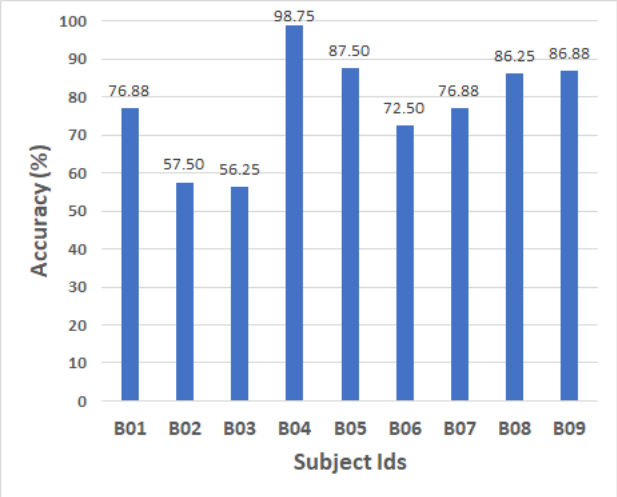

Fig. 5. Classification accuracies of all the subjects in BCI Competition IV-2b dataset using the proposed method with a kernel length of 32 for 100 epochs.

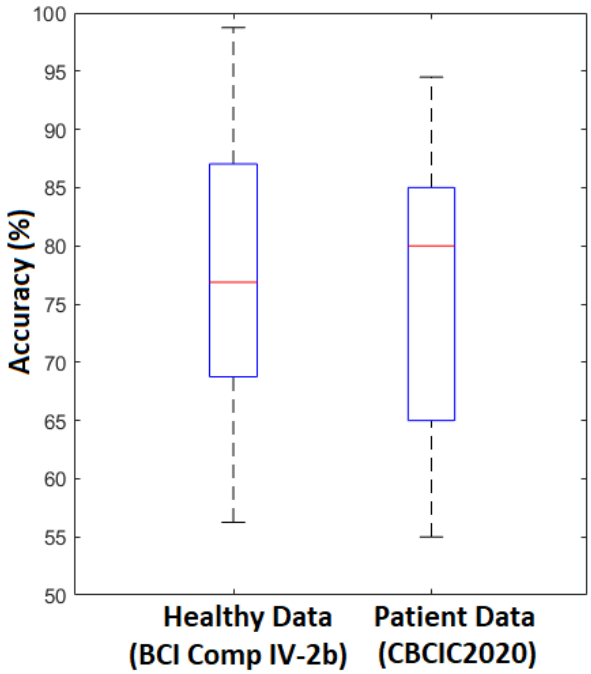

Fig. 6. A comparison of the performance of the proposed method between healthy subjects' and stroke patients' datasets.

IV. Discussion

In the current study, our focus was to emphasize on two major attributes to evaluate a deep learning framework for BCI applications which are largely ignored. The attributes of cross-subject decoding and validating it on stroke patients are particularly important as the major application area of BCI is in rehabilitation and the practical usability of a BCI device is often suffered by repeated calibration. Hence, the validity of an algorithm in cross-subject decoding paves the way for calibration-free BCI systems and it becomes especially effective if it gives a sufficient performance in stroke patients' data.

The proposed method, EEGNET with LCR, was tested for within-subject category with a 2-second window in Table I. The 2-second window is divided into multiple sliding time windows. The classifier was trained to examine the predictions for each sliding time window with different kernel lengths and three distinct epochs were evaluated using the proposed method. Individual participant accuracies are reported in Table I. The highest average accuracy was observed for 500 epochs of training with 66.90%. In this 500 epochs case, seven out of ten participants surpassed the 60% accuracy mark. To achieve the best results, we computed the accuracies by selecting the best sliding time window with an accuracy level exceeding 70%, resulting in an improved accuracy of 76.94% for within-subject classification as reported in Table II and cross-subject classification accuracy of 74.5% as reported in Table III.

In this study, if we look at the cross-subject with the

TABLE I
FREQUENCY RANGE [8-24 HZ],WINDOW SIZE = 2SEC, DROPOUT: 0.25, KERNEL LENGTH = 64 FOR 100 EPOCHS OF TRAINING, KERNEL LENGTH = 32 FOR 300 AND 500 EPOCHS OF TRAINING.

Subject Id	Test Acc(%)	Test Acc(%)	Test Acc(%)
Epochs	**100**	**300**	**500**
S01	85	80	60
S02	47	50	48
S03	57	60	52
S04	57	70	62
S05	70	57.5	50
S06	55	67.5	65
S07	65	67.5	85
S08	50	67.5	75
S09	60	65	87
S10	70	70	85
Mean	61.6	65.5	66.9

TABLE II
WITHIN-SUBJECT CLASSIFICATION ACCURACY WITH THE FOLLOWING PARAMETERS: FREQUENCY RANGE [8-24 HZ], DROPOUT: 0.25, KERNEL LENGTH = 64 FOR 100 EPOCHS OF TRAINING, KERNEL LENGTH = 32 FOR 300 AND 500 EPOCHS OF TRAINING.

Subject ID	Test Acc(%)	Test Acc(%)	Test Acc(%)
Epochs	**100**	**300**	**500**
S01	75	77.5	85
S02	72.5	82.5	85
S03	50	50	77.49
S04	60	57.5	72.5
S05	62.5	65	65
S06	52.6	60	60
S07	92.5	90	92.5
S08	87.5	80	82.5
S09	55	65	55
S10	85	92.5	94.5
Mean	69.26	72	76.94
Std	15.44	14.47	13.5

TABLE III
CROSS-SUBJECT CLASSIFICATION ACCURACY WITH THE FOLLOWING PARAMETERS: FREQUENCY RANGE [8-24 HZ], DROPOUT: 0.25, KERNEL LENGTH = 32 FOR 100 EPOCHS OF TRAINING, KERNEL LENGTH = 128 FOR 300, AND KERNEL LENGTH = 32 FOR 500 EPOCHS OF TRAINING.

Sub ID	Test Acc(%)	Test Acc(%)	Test Acc(%)
Epochs	**100**	**300**	**500**
S01	50	50	52.5
S02	72.5	72.5	82.5
S03	72.5	85	85
S04	55	60	57.5
S05	65	70	69.9
S06	75	55	87.5
S07	62.5	75	90
S08	72.5	77.5	60
S09	62.5	60	70
S10	87.5	92.5	90
Mean	67.5	69.75	74.5
Std	10.8	13.51	14.33

TABLE IV
VARIATION OF CLASSIFICATION ACCURACY CORRESPONDING TO THE NUMBER OF SLIDING WINDOWS FOR LCR COMPUTATION

	Number of Windows				
SubID	**3**	**4**	**5**	**6**	**7**
B01	75.63	75.63	76.25	75.63	76.88
B02	60.00	60.00	60.00	59.38	57.50
B03	56.25	56.25	54.37	54.37	56.25
B04	98.13	98.13	98.75	98.75	98.75
B05	84.38	84.38	86.88	86.88	87.50
B06	74.38	74.38	72.50	72.50	72.50
B07	76.88	76.88	79.38	79.38	76.88
B08	84.38	84.38	85.00	84.38	86.25
B09	80.00	80.00	86.88	86.88	86.88
Mean	76.67	76.67	77.78	77.57	77.71
Std	12.71	12.71	13.94	14.01	14.11
Median	76.88	76.88	79.38	79.38	76.88

best sliding window selection results for stroke patients we can see that the average decoding accuracy of 74.5% was beyond the threshold of 70% while 40% of the participants achieved a very high accuracy beyond 80%. This is a good indicator of how well it performed for cross-subject decoding on stroke patients. Of course, we calculated the within-subject accuracies with the best sliding window selection for the participants and it was higher (76.94%) than the cross-subject accuracy for obvious reasons that the classifier was trained on the same participant's data on whom it was tested where the variability was much less than the cross-subject case. Here the number of participants performing beyond 80% was at 50% (more than the cross-subject case) while 20% of the participants achieved accuracies beyond 90%. Most importantly, we observed no statistically significant ($p-$value = 0.7812) difference between the within-subject performance and cross-subject performance measured by Wilcoxon signed rank test. This is an interesting observation as most often it was observed that the same algorithm do not perform equally well in both within-subject and cross-subject cases as evident in 'CBCIC 2020' [33]. In the 'CBCIC 2020' competition we have seen that the winning algorithm (Riemmanian manifold+functional connectivity+ensemble learning) in the within-subject category didn't perform sufficiently well in the cross-subject category while the winning algorithm (FBCSP + single electrode energy features (SEE)+ evolutionary optimization) in cross-subject category gave only moderate performance in the within-subject case. Therefore, the augmentation of EEGNet using LCR is a promising candidate for a decoding technique that can cover both categories.

Moreover, if we consider the proposed technique with its predecessor i.e. only EEGNet without LCR, we can see that it outperformed the accuracy reported in [36] in both within- and cross-subject categories (Fig. 4) For the within-subject case we got a performance improvement of +6.69% while in cross-subject case the performance improvement is at +10%. The effect size in the case of within-subject performance improvement was medium (Cohen's d = 0.44) while in the case of cross-subject, the performance improvement of a large

effect size (Cohen's d = 0.74) is observed. This shows that the technique of LCR-based augmentation of EEGNet is an effective way to improve its performance. In comparison to the traditional method of CSP+support vector machine (SVM) based classification as reported in [34] the average decoding accuracy improved by +6.69% with a large effect size (Cohen's d = 0.68). The cross-subject accuracy for CSP+SVM was also computed to be 70.25% which is 4.24% lower than the proposed approach although the effect size is found to be moderate (Cohen's d = 0.38).

There are also some non-traditional techniques of MI decoding such as the Riemannian geometry (RG) based approach which was used in conjunction to EEGNet in 'CB-CIC 2020'. The technique of RG+EEGNet achieved 73.75% average decoding accuracy which is 3.19% less than the proposed EEGNet+LCR technique. In addition to that, the implementation LCR is much simpler than RG and less time-consuming which makes the former a better choice for augmenting EEGNet performance. The EEGNet+LCR also performed better than CSP+LCR reported in [32] with +3.44% improvement in average accuracy. We have compared our results of the BCI competition IV-2b dataset with other deep learning architectures on the same dataset. For example, Roy et al. [37] presented results on BCI Competition IV-2b dataset using a Mega-Block based CNN architecture using Adam and SGDM training methods which yielded an average accuracy of 72.63% and 73.13% accordingly, while the proposed method performed with a significantly ($p-$value<0.05) higher accuracy at 77.71%. This result is also +2.71% higher than the CNN architecture proposed in [8] which resulted in an average accuracy of 75%. As compared to SVM on time-frequency features (average accuracy = 72.4% [8]) the proposed method achieved an improvement of 5.3%. Moreover, the advantage of using the proposed method it does not require customized features as in [8] and [37] as the features can be learned from the raw data only.

A comparison between the healthy subjects' and stroke patients' performance can be seen in Fig. 6 in the form of a box plot. The average accuracy for stroke patients is 76.94% and for healthy subjects, it is 77.71%, while no significant difference in performance was seen between the two. This shows the robustness of the proposed method to be a generalized solution for both healthy and stroke patients which is rarely found in the literature.

Apart from these encouraging results we also kept some essential elements in our approach so that the current benchmark can be tested further when new data on stroke patients' MI is available or some new methods emerge. For example, unlike some previous studies which were focused on cross-validation accuracies on the same session ([8], [15], [21]) our focus was on session-to-session transfer. The issue of generalizability is perhaps the most ignored issue in the MI-BCI literature except a few [19], [15], [27]. Hence, we emphasised on cross-subject decoding to establish the generalizability of the proposed technique. Additionally, the literature is really scarce when it comes to cross-subject decoding on stroke patients which can be the most challenging as the inter-subject variability is significantly higher in the case of stroke patients due to altered neurodynamics after stroke. Hence, while choosing the validation criteria for the proposed technique we went to testing its performance on cross-subject decoding of stroke patients' data. Because our approach includes a deep learning network we believed that the best way to make use of this emerging technique is to go for automated feature extraction by the network rather than going for deep learning networks using handcrafted features [25], [8], [21]. This was the reasoning behind the choice of EEGNet which is an end-to-end deep learning framework specially tested for its generalizability. The performance of EEGNet+LCR was also compared against both conventional and non-conventional techniques on both within- and cross-subject categories which should serve as a solid benchmark for future reference as a majority of the previous studies only reported only a subset of these aspects.

The fact that the dataset used in this paper is generated out of an actual neurorehabilitation paradigm with the modern technique of using hand-exoskeleton makes the results especially relevant for robotic control. This is because to the best of the authors' knowledge, it is for the first time that a EEGNet-based MI decoding is tested on a robotic rehabilitation paradigm on stroke patients. As the proposed technique takes a sliding window-based approach in a single trial framework the paradigm can be redesigned for continuous control of the robotic exoskeleton using the same technique of decoding which can be a scope for future research. Another direction of further improvement can be the adaptation of the classifier trained on other subjects' data when fresh data from a new subject is available online. The future work can also include a study of the proposed EEGNet+LCR technique on the magnetoencephalography (MEG) dataset to see its applicability across different brain signal modalities other than EEGNet. This is particularly important as it is a big challenge to apply deep learning-based architectures on very high-dimensional datasets such as MEG where more than 300 channels are available.

In this paper the proposed method is applied only to stroke patients. However, there is a large similarity between the signals of stroke patients and some other neurological diseases such as traumatic brain injuries (TBI) which indicates that the proposed method should work in those cases too. As such datasets are very rare to find related to BCI experiments we have future plans to conduct similar studies on TBI patients to acquire new data.

V. Conclusion

In this paper, we have introduced a new technique for augmenting the performance of EEGNet architecture using LCR. The proposed EEGNet+LCR based technique was tested for the first time for cross-subject decoding on stroke patients dataset involving BCI-based hand-exoskeleton as a rehabilitation paradigm. The results have outperformed many of the competitive algorithms ranging from conventional to non-conventional used in BCI-based neurorehabilitation paradigms which paved the way for realizing calibration-free BCI designs in practical scenarios. It was also encouraging to observe that it performed equally well not only in both within- and cross-subject decoding frameworks but also for both healthy and

stroke patients' datasets which is rarely found in the literature. Overall, the study shows a promising way to leverage the performance of a generalizable deep learning architecture that could enhance the usability of BCI-based robotic rehabilitation.

REFERENCES

[1] H. Raza, A. Chowdhury, and S. Bhattacharyya, "Deep learning based prediction of eeg motor imagery of stroke patients' for neuro-rehabilitation application," in *2020 International Joint Conference on Neural Networks (IJCNN)*. IEEE, 2020, pp. 1–8.

[2] S. Sakhavi, C. Guan, and S. Yan, "Parallel convolutional-linear neural network for motor imagery classification," in *2015 23rd European Signal Processing Conference (EUSIPCO)*. IEEE, 2015, pp. 2736–2740.

[3] K. K. Ang, Z. Y. Chin, C. Wang, C. Guan, and H. Zhang, "Filter bank common spatial pattern algorithm on bci competition iv datasets 2a and 2b," *Frontiers in neuroscience*, vol. 6, p. 39, 2012.

[4] L. Zheng, Y. Ma, P. Lian, Y. Xiao, Z. Yi, Q. Song, W. Feng, and X. Wu, "A power spectrum pattern difference-based time-frequency sub-band selection method for mi-eeg classification," *IEEE Sensors Journal*, 2022.

[5] N. Lu, T. Li, X. Ren, and H. Miao, "A deep learning scheme for motor imagery classification based on restricted boltzmann machines," *IEEE transactions on neural systems and rehabilitation engineering*, vol. 25, no. 6, pp. 566–576, 2016.

[6] F. Paissan, V. P. Kumaravel, and E. Farella, "Interpretable cnn for single-channel artifacts detection in raw eeg signals," in *2022 IEEE Sensors Applications Symposium (SAS)*. IEEE, 2022, pp. 1–6.

[7] Z. Tang, C. Li, and S. Sun, "Single-trial eeg classification of motor imagery using deep convolutional neural networks," *Optik*, vol. 130, pp. 11–18, 2017.

[8] Y. R. Tabar and U. Halici, "A novel deep learning approach for classification of eeg motor imagery signals," *Journal of neural engineering*, vol. 14, no. 1, p. 016003, 2016.

[9] R. T. Schirrmeister, J. T. Springenberg, L. D. J. Fiederer, M. Glasstetter, K. Eggensperger, M. Tangermann, F. Hutter, W. Burgard, and T. Ball, "Deep learning with convolutional neural networks for eeg decoding and visualization," *Human brain mapping*, vol. 38, no. 11, pp. 5391–5420, 2017.

[10] T. Shi, L. Ren, and W. Cui, "Feature extraction of brain–computer interface electroencephalogram based on motor imagery," *IEEE Sensors Journal*, vol. 20, no. 20, pp. 11 787–11 794, 2019.

[11] J. Jin, Z. Wang, R. Xu, C. Liu, X. Wang, and A. Cichocki, "Robust similarity measurement based on a novel time filter for ssveps detection," *IEEE Transactions on Neural Networks and Learning Systems*, pp. 1–10, 2021.

[12] J. Jin, R. Xiao, I. Daly, Y. Miao, X. Wang, and A. Cichocki, "Internal feature selection method of csp based on l1-norm and dempster–shafer theory," *IEEE Transactions on Neural Networks and Learning Systems*, vol. 32, no. 11, pp. 4814–4825, 2021.

[13] M. Xu, J. Han, Y. Wang, T.-P. Jung, and D. Ming, "Implementing over 100 command codes for a high-speed hybrid brain-computer interface using concurrent p300 and ssvep features," *IEEE Transactions on Biomedical Engineering*, vol. 67, no. 11, pp. 3073–3082, 2020.

[14] Q. Yao, H. Gu, S. Wang, and X. Li, "A feature-fused convolutional neural network for emotion recognition from multichannel eeg signals," *IEEE Sensors Journal*, 2022.

[15] V. J. Lawhern, A. J. Solon, N. R. Waytowich, S. M. Gordon, C. P. Hung, and B. J. Lance, "Eegnet: a compact convolutional neural network for eeg-based brain–computer interfaces," *Journal of neural engineering*, vol. 15, no. 5, p. 056013, 2018.

[16] S. Sakhavi, C. Guan, and S. Yan, "Learning temporal information for brain-computer interface using convolutional neural networks," *IEEE transactions on neural networks and learning systems*, vol. 29, no. 11, pp. 5619–5629, 2018.

[17] K. Samanta, S. Chatterjee, and R. Bose, "Cross-subject motor imagery tasks eeg signal classification employing multiplex weighted visibility graph and deep feature extraction," *IEEE Sensors Letters*, vol. 4, no. 1, pp. 1–4, 2019.

[18] E. Dagois, A. Khalaf, E. Sejdic, and M. Akcakaya, "Transfer learning for a multimodal hybrid eeg-ftcd brain–computer interface," *IEEE Sensors Letters*, vol. 3, no. 1, pp. 1–4, 2018.

[19] O.-Y. Kwon, M.-H. Lee, C. Guan, and S.-W. Lee, "Subject-independent brain–computer interfaces based on deep convolutional neural networks," *IEEE transactions on neural networks and learning systems*, vol. 31, no. 10, pp. 3839–3852, 2019.

[20] S. Mohdiwale, M. Sahu, G. Sinha, and V. Bhateja, "Statistical wavelets with harmony search-based optimal feature selection of eeg signals for motor imagery classification," *IEEE Sensors Journal*, vol. 21, no. 13, pp. 14 263–14 271, 2020.

[21] F. Li, F. He, F. Wang, D. Zhang, Y. Xia, and X. Li, "A novel simplified convolutional neural network classification algorithm of motor imagery eeg signals based on deep learning," *Applied Sciences*, vol. 10, no. 5, p. 1605, 2020.

[22] B. E. Olivas-Padilla and M. I. Chacon-Murguia, "Classification of multiple motor imagery using deep convolutional neural networks and spatial filters," *Applied Soft Computing*, vol. 75, pp. 461–472, 2019.

[23] G. Dai, J. Zhou, J. Huang, and N. Wang, "Hs-cnn: a cnn with hybrid convolution scale for eeg motor imagery classification," *Journal of neural engineering*, vol. 17, no. 1, p. 016025, 2020.

[24] Y. Li, X.-R. Zhang, B. Zhang, M.-Y. Lei, W.-G. Cui, and Y.-Z. Guo, "A channel-projection mixed-scale convolutional neural network for motor imagery eeg decoding," *IEEE Transactions on Neural Systems and Rehabilitation Engineering*, vol. 27, no. 6, pp. 1170–1180, 2019.

[25] X. Zhao, H. Zhang, G. Zhu, F. You, S. Kuang, and L. Sun, "A multi-branch 3d convolutional neural network for eeg-based motor imagery classification," *IEEE transactions on neural systems and rehabilitation engineering*, vol. 27, no. 10, pp. 2164–2177, 2019.

[26] Z. Tayeb, J. Fedjaev, N. Ghaboosi, C. Richter, L. Everding, X. Qu, Y. Wu, G. Cheng, and J. Conradt, "Validating deep neural networks for online decoding of motor imagery movements from eeg signals," *Sensors*, vol. 19, no. 1, p. 210, 2019.

[27] R. Zhang, Q. Zong, L. Dou, and X. Zhao, "A novel hybrid deep learning scheme for four-class motor imagery classification," *Journal of neural engineering*, vol. 16, no. 6, p. 066004, 2019.

[28] T.-j. Luo, C.-l. Zhou, and F. Chao, "Exploring spatial-frequency-sequential relationships for motor imagery classification with recurrent neural network," *BMC bioinformatics*, vol. 19, no. 1, pp. 1–18, 2018.

[29] Y. Zhang, S. Q. Xie, H. Wang, and Z. Zhang, "Data analytics in steady-state visual evoked potential-based brain–computer interface: A review," *IEEE Sensors Journal*, vol. 21, no. 2, pp. 1124–1138, 2020.

[30] P. Autthasan, X. Du, J. Arnin, S. Lamyai, M. Perera, S. Itthipuripat, T. Yagi, P. Manoonpong, and T. Wilaiprasitporn, "A single-channel consumer-grade eeg device for brain–computer interface: Enhancing detection of ssvep and its amplitude modulation," *IEEE Sensors Journal*, vol. 20, no. 6, pp. 3366–3378, 2019.

[31] S. Zhang, Z. Zhu, B. Zhang, B. Feng, T. Yu, and Z. Li, "Fused group lasso: A new eeg classification model with spatial smooth constraint for motor imagery-based brain–computer interface," *IEEE Sensors Journal*, vol. 21, no. 2, pp. 1764–1778, 2020.

[32] P. Gaur, H. Gupta, A. Chowdhury, K. McCreadie, R. B. Pachori, and H. Wang, "A sliding window common spatial pattern for enhancing motor imagery classification in eeg-bci," *IEEE Transactions on Instrumentation and Measurement*, vol. 70, pp. 1–9, 2021.

[33] A. Chowdhury and J. Andreu-Perez, "Clinical brain-computer interface challenge 2020 (cbcic at wcci2020): Overview, methods and results," *IEEE Transactions on Medical Robotics and Bionics*, 2021.

[34] A. Chowdhury, H. Raza, Y. K. Meena, A. Dutta, and G. Prasad, "Online covariate shift detection-based adaptive brain–computer interface to trigger hand exoskeleton feedback for neuro-rehabilitation," *IEEE Transactions on Cognitive and Developmental Systems*, vol. 10, no. 4, pp. 1070–1080, 2017.

[35] M. Tangermann *et al.*, "Review of the bci competition iv," *Frontiers in Neuroscience*, vol. 6, 2012.

[36] H. Raza, A. Chowdhury, and S. Bhattacharyya, "Deep learning based prediction of eeg motor imagery of stroke patients' for neuro-rehabilitation application," in *2020 International Joint Conference on Neural Networks (IJCNN)*. IEEE, 2020, pp. 1–8.

[37] S. Roy, A. Chowdhury, K. McCreadie, and G. Prasad, "Deep learning based inter-subject continuous decoding of motor imagery for practical brain-computer interfaces," *Frontiers in Neuroscience*, vol. 14, 2020.